^{13}C NMR Spectral Characterization of Epimeric Rotenone and Some Related Tetrahydrobenzopyranofurobenzopyranones

S. L. Abidi [1]

U. S. Fish and Wildlife Service, National Fishery Research Laboratory,
P. O. Box 818, La Crosse, Wisconsin 54601

M. S. Abidi

Department of Chemistry, Catholic University of America,
Washington D. C. 20064

Received May 9, 1983

The ^{13}C nuclear magnetic resonance (nmr) spectra of epimers of rotenone and four 12a-hydroxy-analogues were examined to determine the stereochemical effect of the B/C ring fusion involving the 6a- and 12a-carbon centers. Chemical shift differences between the epimeric carbon resonances of *cis*- and *trans*-6a,12a-compounds were notably larger than those of diastereoisomers derived from the same B/C ring junction stereochemistry. Results of the spectral analysis have been useful for the quantification of mixtures of epimers and for the measurement of rates of epimerization and oxygenation.

J. Heterocyclic Chem., **20**, 1687 (1983).

Introduction.

Rotenone (**IA**), the prototype in the series of title compounds investigated in this study (Figure 1), is a naturally occurring substance and a well-known agricultural insecticide and fish toxicant. Because of the presence of a highly reactive site in its molecule at the 12a-position and labile functionalities elsewhere that contribute to its nonpersistence, rotenone degrades rapidly in the environment to a diversity of comparatively polar, but less toxic, materials. Recently, we reported on the environmental fate as well as degradation kinetics of structure **IA** as shown in Figure 1 and related analogues [2]. By using high-performance liquid chromatography (hplc), we were able to follow quantitatively the rates of formation of the 6aα, 12aα-epimer (**IB**), from **IA** through initial enolization and the rates of oxygenation of **IA** and **IB** to yield respective rotenolones **IIA** and **IIB** (Figure 1). We have found that, under mildly alkaline conditions simulating the natural environment, **IB** undergoes oxidation faster than **IA**. Apart from the epimeric **IIA** and **IIB** constituting the major products, air

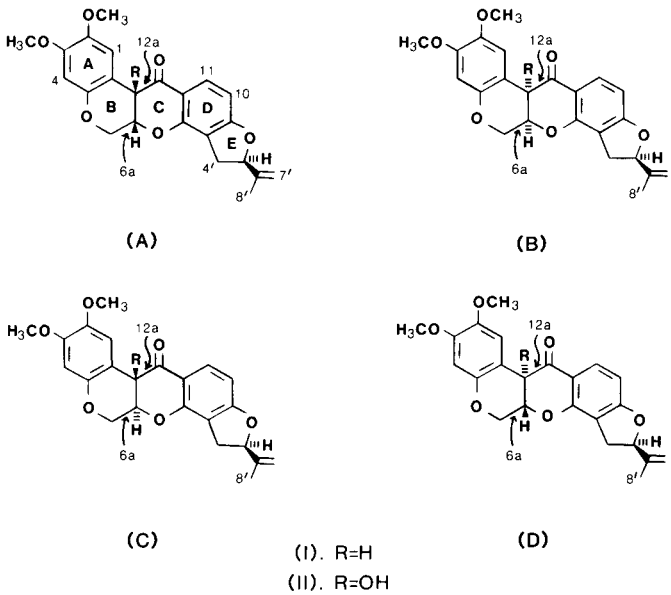

Figure 1. Structures of the six rotenone-related compounds (tetrahydrobenzopyranofurobenzopyranones).

Table I

^{13}C NMR Chemical Shifts of Type **I** Compounds

Carbon	Chemical Shift, δ (ppm) [a] Compound **IA**	**IB**	**IA** (H)	$\Delta\delta$ [b]
1	110.1 (d)	110.1 (d)	112.3 (d)	—
2	157.4 (s)	157.4 (s)	159.1 (s)	—
3	166.8 (s)	166.8 (s)	168.8 (s)	—
4	100.6 (d)	100.6 (d)	102.4 (d)	—
4a	143.4 (s)	143.4(s)	145.2 (s)	—
4′	30.9 (t)	30.9 (t)	30.6 (t)	—
5′	87.3 (d)	87.6 (d)	91.9 (d)	0.3
6	65.9 (t)	65.9 (t)	67.5 (t)	—
6a	71.8 (d)	72.1 (d)	73.5 (t)	0.3
6′	142.6 (s)	142.6 (s)	34.4 (d)	—
7a	147.0 (s)	147.0 (s)	148.8 (s)	—
7′	112.5 (t)	112.1 (t)	18.7 (q)	0.4
8	112.9 (s)	112.9 (s)	114.3 (s)	—
8′	16.7 (q)	16.7 (q)	19.1 (q)	—
9	149.0 (s)	149.0 (s)	150.9 (s)	—
10	104.4 (d)	104.4 (d)	105.9 (d)	—
11	129.4 (d)	129.4 (d)	130.9 (d)	—
11a	113.1 (s)	113.1 (s)	114.5 (s)	—
12	188.3 (s)	188.3 (s)	190.0 (s)	—
12a	44.1 (d)	44.1 (d)	45.8 (d)	—
12b	104.5 (s)	104.5 (s)	106.4 (s)	—
2-OCH_3 [c]	55.3 (q)	55.3 (q)	57.1 (q)	—
3-OCH_3 [c]	55.9 (q)	55.9 (q)	57.6 (q)	—

[a] Chemical shifts in parts per million (ppm) from internal TMS for solution in deuterated chloroform; letters in parentheses represent spin multiplicities: s = singlet, d = doublet, t = triplet, and q = quartet; accuracy, ± 0.03 ppm. [b] $\Delta\delta$ = chemical shift difference between the epimeric pair of carbon resonances of **IA** and **IB**. [c] Assignments can be reversed.

oxygenation of the natural rotenone **IA** produced two additional minor components **IIC** and **IID**, in which the 6a- and 12a-carbons assume the *trans* relation illustrated in Figure 1. Although there is a vast volume of literature [3] on chemical transformations and biological interactions of rotenone, no published reports pertain to the qualitative and quantitative treatment on the structures and dynamic aspects of epimeric rotenone compounds by ^{13}C nmr spectrometry. In light of the reported apparent relationship between B/C ring junction stereochemistry and the potency of the inhibition of mitochondrial respiratory activity demonstrated by numerous rotenoids [4], it would be desirable to know the exact composition of given epimeric mixtures so that the degree of potency in biological activity in test specimens can be estimated.

This study had two purposes: First, to determine the chemical shifts of all carbons in rotenone (**IA**) and its epimer (**IB**), and in the related 12a-hydroxylated compounds **IIA, IIB, IIC**, and **IID** (Figure 1); and second, to ascertain the extent of differentiability between the carbon resonances of epimeric pairs for analytical application (determination of epimeric ratios).

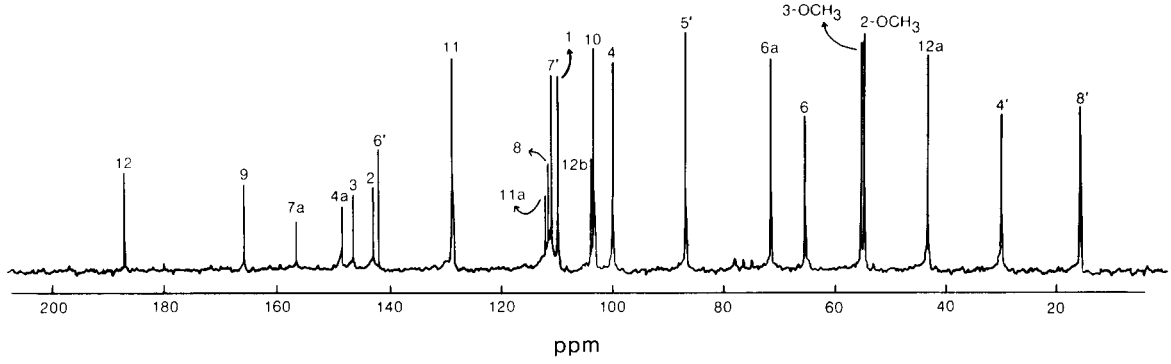

Figure 2. Proton noise-decoupled Fourier transform ^{13}C nmr spectrum of **IA** at 22.5 MHz.

Table II

^{13}C NMR Chemical Shifts of Type **II** Compounds

Carbon	Chemical Shift, δ (ppm) [a] Compound **IIA**	**IIB**	**IIC**	**IID**	$\Delta\delta^1$	$\Delta\delta^2$	$\Delta\delta^3$ [b]
1	109.7 (d)	109.7 (d)	112.4 (d)	112.4 (d)	—	—	2.7
2	157.3 (s)	157.3 (s)	156.7 (s)	156.7 (s)	—	—	0.6
3	167.6 (s)	167.6 (s)	166.7 (s)	166.7 (s)	—	—	0.9
4	100.9 (d)	100.9 (d)	100.5 (d)	100.5 (d)	—	—	0.4
4a	143.7 (s)	143.7 (s)	143.6 (s)	143.6 (s)	—	—	0.1
4'	30.8 (t)	31.1 (t)	31.2 (t)	31.4 (t)	0.3	0.2	0.4
5'	87.6 (d)	87.9 (d)	87.8 (d)	88.2 (d)	0.3	0.4	0.2
6	63.5 (t)	63.5 (t)	61.5 (t)	61.5 (t)	—	—	2.0
6a	75.7 (d)	76.2 (d)	76.6 (d)	76.9 (d)	0.5	0.3	0.9
6'	142.6 (s)	142.6 (s)	142.9 (s)	142.9 (s)	—	—	0.3
7a	148.2 (s)	148.2 (s)	149.4 (s)	149.4 (s)	—	—	1.2
7'	111.7 (t)	111.4 (t)	112.6 (t)	112.2 (t)	0.3	0.4	0.9
8	112.7 (s)	112.7 (s)	113.5 (s)	113.5 (s)	—	—	1.3
8'	16.8 (q)	16.8 (q)	17.0 (q)	17.0 (q)	—	—	0.2
9	150.9 (s)	150.9 (s)	151.1 (s)	151.1 (s)	—	—	0.2
10	104.9 (d)	104.9 (d)	105.1 (d)	105.1 (d)	—	—	0.2
11	129.8 (d)	129.8 (d)	130.8 (d)	130.8 (d)	—	—	1.0
11a	112.2 (s)	112.2 (s)	114.3 (s)	114.3 (s)	—	—	2.1
12	190.8 (s)	190.8 (s)	187.3 (s)	187.3 (s)	—	—	3.5
12a	67.3 (s)	67.3 (s)	66.0 (s)	66.0 (s)	—	—	1.3
12b	108.5 (s)	108.5 (s)	110.1 (s)	110.1 (s)	—	—	1.6
2-OCH_3 [c]	55.4 (q)	55.4 (q)	55.6 (q)	55.6 (q)	—	—	0.2
3-OCH_3 [c]	56.0 (q)	56.0 (q)	56.3 (q)	56.3 (q)	—	—	0.3

[a] Experimental conditions and other details are same as in Table I. [b] $\Delta\delta^1$ = chemical shift difference between epimeric carbon resonances of **IIA** and **IIB**; $\Delta\delta^2$ = chemical shift difference between epimeric carbon resonances of **IIC** and **IID**; $\Delta\delta^3$ = chemical shift difference between epimeric carbon resonances of **IIA** and **IIC**. [c] Assignments can be reversed.

Table III

Spin Lattice Relaxation Times (T_1) of Epimeric Carbons of Analytical Interest [a]

Carbon	Relaxation time, T_1, (sec) Compound IA	IB	IIA	IIB	IIC	IID
4'	0.242	0.240	0.263	0.259	0.237	0.241
5'	0.534	0.527	0.498	0.511	0.509	0.512
6a	0.391	0.400	0.420	0.417	0.386	0.379
8	8.111	8.113	7.898	7.915	8.204	8.203
11a	11.62	11.65	10.69	10.73	10.36	10.27

[a] Measured at 22.5 MHz, 30°, 0.6*M* solution in deuterated chloroform. Coefficient of variation for T_1 determinations, 2-6%.

Results and Discussion.

On the basis of the chemical shift, spin lattice relaxation time, substituent effect, and proton coupled and decoupled spectral considerations, we elaborated the first detailed spectral assignment for the seven compounds **IA, IB, IA(H), IIA, IIB, IIC**, and **IID** of the title five-fused-ring structure. The 6',7'-dihydro-analogue (**IA**[H]) of natural (6aβ,12aβ-) rotenone (**IA**) was included in the study to confirm assignment of the 6'- and 7'- olefinic carbon resonances in rotenone. The proton noise-decoupled natural abundance ^{13}C spectrum of **IA** (Figure 2) shows that, except for a few peaks in the low-field region, nearly all carbons of **IA** give adequately dispersed signals in the spectrum. The spectra of the rest of the series exhibit similar features (Figures 3-4). The chemical shift and spin multiplicity data obtained from these spectral analyses are compiled in Tables I and II.

Using the single-frequency off-resonance proton decoupling technique, we readily assigned chemical shift values to the saturated carbons (in the region 0-100 ppm) on the three heterocyclic rings (B, C, and E [Figure 1]) and the 5'-side chain by analyzing C-H splitting patterns (Tables I and II) and applying chemical shift principles.

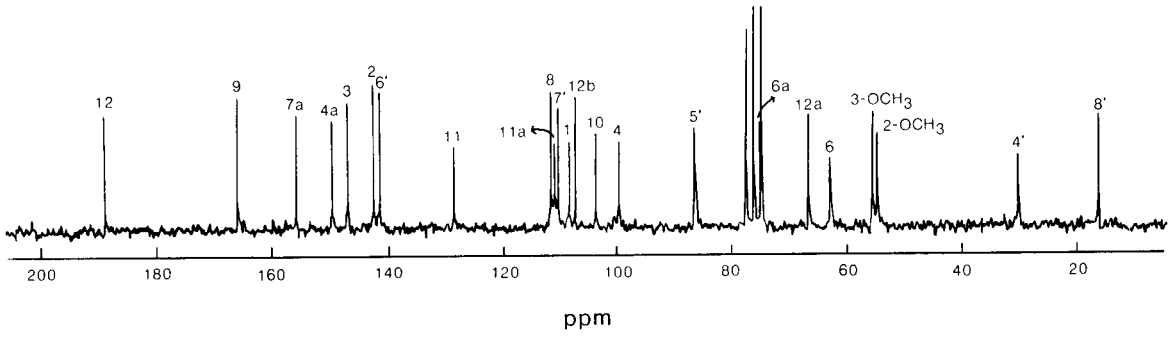

Figure 3. Proton noise-decoupled Fourier transform ^{13}C nmr spectrum of **IIA** at 22.5 MHz.

Table IV

One-Bond ^{13}C-^1H Coupling Constants ($^1J_{C-H}$) and Relevant ^1H Resonances of Representative Compounds [a]

Carbon	Compound IA $^1J_{C-H}$	IA ^1H, δ	IIA $^1J_{C-H}$	IIA ^1H, δ	IIC $^1J_{C-H}$	IIC ^1H, δ
1	160.2	6.76	155.7	6.55	157.1	7.77
4	158.8	6.37	158.6	6.41	158.6	6.32
4'	133.7	2.91	135.7	2.89	134.7	2.96
5'	143.0	5.02	144.4	5.18	142.9	5.30
6	154.4	4.15	148.5	4.55	148.0	4.52
6a	151.5	4.87	152.9	4.61	144.3	4.92
7'	158.4	4.85	156.5	4.87	155.7	4.90
8'	130.0	1.71	128.6	1.70	127.7	1.74
10	165.9	6.46	162.9	6.49	164.3	6.58
11	165.6	7.81	164.3	7.80	162.9	7.84
12a	136.8	3.71	—	—	—	—
2-OCH_3	144.4	3.75	143.3	3.71	143.3	3.78
3-OCH_3	145.4	3.75	143.9	3.71	144.0	3.78

[a] These individual proton frequencies were used in the selective decoupling experiments to identify the directly coupled or long-range coupled carbons. The δ values for ^1H resonances are in parts per million (ppm) from internal TMS for solution in deuterated chloroform. The values for the coupling constant, $^1J_{C-H}$, are in Hertz units (Hz). Accuracy: ± 0.03 ppm for the proton shift determinations; ± 2 Hz for the coupling constant measurements.

Thus, the chemical shift determined for 2-OCH_3, 3-OCH_3, 4'-, 5'-, 6-, 6a-, 8'-, and 12a-carbons are in good agreement with the published values [5] for similar carbons in analogous structures. The expected downfield shifts ($\Delta\delta$, 21.9-23.2 ppm) experienced by the 6a- and 12a-carbons in type **II**-compounds (**IIA, IIB, IIC**, and **IID**) relative to that in type **I** compounds (**IA, IB**, and **IA**[H]) provide additional confirmatory checks on the signal assignment of all carbons at these two positions in both type **I** and **II** compounds. It is noteworthy that the diastereotopic 7'- and 8'-methyl carbons in **IA**(H) are magnetically nonequivalent. Their chemical shifts are separated by 0.4 ppm (Table I). In some experiments in which dilute sample solutions were used, (Figures 3-4), peak overlaps with solvent (deuteriochloroform) signals within the 75-80 ppm region caused ambiguity in the assignment of chemical shift values to 6a-carbons from the off-resonance decoupled spectra alone. To remove the uncertainty from this shift assignment, we preferably extracted the signals attributable to the 6a-carbons from the single-frequency proton coupled spectra.

Among the 13 aromatic unsturated carbons, we could use simple substituent effect arguments to assign the six lowest field signals to the oxygen-bearing quaternary carbons at positions 12, 9, 7a, 4a, 3, and 2, sequentially from low-field to high-field direction as shown in Figures 2-4. These carbon resonance assignments were corroborated by the sharpening of signals upon irradiation of pertinent proton frequencies in the selective long-range proton decoupling experiments. The 12b-carbon resonances were determined on the basis of observed changes in chemical shift values ($\Delta\delta$, 4.0-5.6 ppm) associated with the subtitution of a hydrogen atom (H) by a hydroxyl-group (OH) at the 12a-carbon center. Since the nuclear Overhauser effect (NOE) of the two narrowly separated signals in the lower field portion, near the 112.2-114.5 ppm region, was experimentally verified to reach the maximum value, we could anticipate that one of the two remaining nonprotonated carbons at the 11a- and 8-positions would require longer relaxation time because of fewer interacting protons in the

Table V

Comparison of Analytical Methods for Determining the Composition of Mixtures of Epimers

		Method [b]			
		^{13}C NMR		HPLC	
No.	Mixture [a]	%	Ratio	%	Ratio
1	IA	61.5	1.59	62.6	1.67
	IB	38.5		37.4	
2	IA	41.3	0.70	38.8	0.63
	IB	58.7		61.2	
3	IIA	50.8	1.03	50.0	1.00
	IIB	49.2		50.0	
4	IIA	39.0	0.64	41.4	0.71
	IIB	61.0		58.6	
5	IIC	71.4	2.50	71.9	2.56
	IID	28.6		28.1	
6	IIC	55.2	1.23	56.1	1.28
	IID	44.8		43.9	
7	IIA	15.3	0.18	16.3	0.19
	IIC	84.7		83.7	
8	IIA	64.7	1.83	65.6	1.91
	IID	35.3		34.4	

[a] Samples were prepared by randomly mixing the pure components. [b] Data are averaged values of triplicate determinations based on the carbon resonance integrals and hplc peak heights. Coefficient of variation: 3-7% for the ^{13}C nmr method; 2-4% for the hplc method.

α-position. For instance, in the spectrum of **IA** (Figure 2), the lower field line at 113.1 ppm with a spin lattice relaxation time (T_1) value of 11.6 sec (Table III) could be designated to the 11a-carbon, and the one slightly upfield at 112.9 ppm (T_1 = 8.11 sec) could accordingly be designated to the 8-carbon [6]. Table III contains T_1 data that aided in the assignment of these two carbons in the various epimeric compounds under study. A positive increase in peak intensity of the 11a- and 8-signals, accompanied by selective decoupling at the respective 12a- and 10-proton frequencies, confirmed the assignment. Initially we assigned the four remaining carbon resonances to the aromatic methine carbons at positions 1, 4, 10, and 11 after carefully examining the aromatic substitution pattern on the A and D rings. These assignments were subsequently sup-

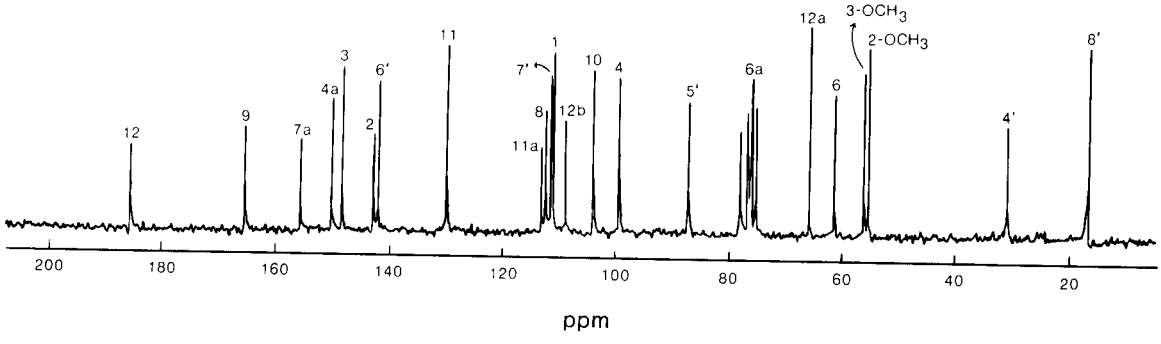

Figure 4. Proton noise-decoupled Fourier transform ^{13}C nmr spectrum of **IIC** at 22.5 MHz.

ported by selective decoupling results, and thus unequivocally established the shift assignment for these methine carbons. Selective irradiation of the specific protons 1, 4, 10, and 11 at their individual frequencies decoupled the corresponding carbon signals to four lines (from eight lines in the single-frequency proton coupled ^{13}C spectra) in the region between 100 and 131 ppm. The proton (^1H) resonances used in all studies are listed in Table IV.

Inasmuch there are three asymmetric centers at 5'-, 6a-, and 12a-carbons in each of the three epimeric pairs of compounds (Figure 1), all structurally related to the natural rotenone (**IA**), the chemical shifts differences ($\Delta\delta$, 0.2-0.5 ppm; Tables I and II) between a limited number of epimeric carbons (three pairs for type **I** and four pairs for type **II**) are generally small but are nevertheless real due to the asymmetric environments produced by the three asymmetric centers. This is particularly true when epimers of the same B/C ring fusion (the 6a- and 12a-substituents are either *cis*- or *trans*- with respect to each other) are compared, as in Table I (column "$\Delta\delta$" for **IA** *vs* **IB**) and Table II (columns "$\Delta\delta^1$" and "$\Delta\delta^2$" for **IIA** *vs* **IIB** and **IIC** *vs* **IID**, respectively). Within this system of ring junction stereochemistry, the 5'-, 6a-, and 7'-carbons in both type **I** and type **II** compounds are consistently implicated in the differentiation of ^{13}C spectral characteristics between the epimers concerned, although an additional epimeric pair of 4'-carbons in type **II** compounds is also resolvable. In general, the saturated carbons on the dihydrofuran moiety (ring-E) seem to have a partial influence on the differentiability in the stereochemical system. In contrast, the "$\Delta\delta^3$" in Table II suggest that epimers of different B/C ring fusion (**IIA** *vs* **IIC** [$\Delta\delta^3$ values are shown in the table for this pair only], **IIA** *vs* **IID**, **IIB** *vs* **IIC**, and **IIB** *vs* **IID**) show relatively greater differential effects on the chemical shifts of all the epimeric carbons (23 pairs), and that a broader spectrum of variations in chemical shift differences ($\Delta\delta^3$,0.1-3.5 ppm) is indicated. The 12-, 1-, 11a-, 6-, 12b-, 12a-, 7a-, and 6a-carbons situated in the proximity of the 6a,12a-ring junction involving the B and C rings are affected in their magnetic environment to a higher degree than are other remote carbons as reflected in the greater magnitude of the chemical shift differences ($\Delta\delta^3$ in Table II). From the Dreiding molecular models, the A and D aromatic rings are seen to be in the nearly coplanar arrangement, falling with the deshielding zone of the 12-carbonyl in a *trans* B/C conformation of **IIC**. This can explain the observed downfield shifts of the carbons at 1-, 7a-, 8-, 11-, 11a-, 12a-, and 12b-positions relative to the epimeric counterparts in the *cis* B/C compound **IIA**. Interestingly, the carbonyl carbon in **IIC** is more shielded than that in **IIA**, presumably due to the shielding effect of proximal protons in **IIC**. In the preferred conformation [7], the molecule of **IIC** can be envisioned to assume a half-chair conformation in which both the 6- and 6a-carbons on the oxygen-containing rings (B and C) are puckered up (as revealed from the model), forcing the 12a-hydroxyl group to be in plane with the 12-carbonyl. This situation would give rise to the higher field chemical shifts of 6- and 6a-carbons of **IIC** in comparison with that of **IIA**, apparently as a result of steric shift.

Table IV compares the one-bond coupling constants ($^1J_{C-H}$) of three typical rotenone compounds representing the three sets of epimers. The experimental data for their epimeric compounds **IB**, **IIB**, and **IID** have been omitted because the results are nearly identical within each set. A cursory survey of the data in Table IV makes it immediately obvious that the coupling constants, $^1J_{C-H}$, of 1-, 6-, and 6a-carbons are somewhat dependent on the stereochemistry of the B/C ring junction. For these carbons, the ^1J-values of the 1- and 6-carbons appear to be sensitive to the change in polarity at the 12a-carbon center (interconversion of a hydroxyl group with a hydrogen atom at this position), whereas the ^1J-values of the 6a-carbons tend to be susceptible to stereochemical modification at the B/C ring junction. In this context, the coupling constants for the rest of the carbons remained essentially unaffected. The magnitudes of the couplings of various carbons in each compound should be of diagnostic value for the study of ring structures in this class of compounds.

The unambiguous assignments of all chemical shifts for the three sets (**IA-IB**, **IIA-IIB**, and **IIC-IID**) of epimeric compounds enabled the identification of the specific carbon resonances that are distinguishable for pairs of carbons at equivalent positions ($\Delta\delta$, $\Delta\delta^1$, $\Delta\delta^2$, and $\Delta\delta^3$ in Tables I-II). Employing a high-resolution instrument, we were able, on the basis of the information on chemical shift difference, to estimate the composition of epimeric mixtures directly from the peak intensity ratios. The two epimeric carbons in a given pair of compounds can be assumed to have the same NOE and relaxation behavior because their environments are similar. This assumption was experimentally substantiated during our NOE and T_1 studies. Results from T_1 measurements (Table III) show the close T_1 values for similar carbons, including those of a different B/C ring fusion. Additional evidence for the reliability of the quantitative analysis is provided by data on intensity ratio obtained by gated-decoupling [8]. Descrepancies in the integral ratios measured by the two methods (with and without gated-decoupling) were insignificant. We have extended the ^{13}C nmr method to kinetic studies on the epimerization and oxygenation of **IA** (not described here). Comparisons of the ^{13}C nmr results with hplc data [2] for the determination of the composition of epimeric mixtures show good agreement (Table V). The biological activity of an unknown sample can be predicted by determining the composition of the sample and using a standard curve that correlates the activity with composition parameters.

EXPERIMENTAL

Natural abundance ^{13}C nmr spectra were obtained at a 30° probe temperature with JEOL Model FX Fourier transform nuclear magnetic resonance spectrometers operating at 22.5 and 67.8 MHz. All chemical shifts are reported in parts per million (ppm) as δ values relative to the internal tetramethylsilane (TMS) standard. Sample solutions in deuteriochloroform (0.1-1.0*M*) were freshly prepared before analyses. Spectra were obtained with the following instrumental parameters: repetition time, 15-20 sec; accumulation, 500-1,000 transients; 60° pulse width, 15 μsec; acquisition time, 0.9 sec; data point, 8K (16K at 67.8 MHz); spectral width, 5,000 Hz (15,000 Hz at 67.8 MHz); resolution, 0.03 ppm; accuracy, 0.03 ppm.

Spin lattice relaxation times (T_1) were determined using the inversion recovery method of Vold, *et al.* [9]. A gated-decoupling technique was employed for NOE measurements (pulse delay, 100 sec used in NOE retention experiments) and for the determination of some intensity ratios.

The ^1H nmr spectra (for selective decoupling) were obtained with the same instrumentation as used to obtain the ^{13}C nmr spectra.

Rotenone (**IA**) was purchased from Aldrich Chemical Company. All other compounds were prepared at the National Fisherey Research Laboratory, La Crosse, Wisconsin, by known procedures [7]. Spectroscopically pure samples of these compounds were obtained by preparative hplc [2].

The melting point data for all the compounds studied are recorded as follows (values in parentheses are the melting points reported in the literature [7]): 6aβ,12aβ-rotenone (**IA**), mp 163-164° (162°); 6aα,12aα-rotenone (**IB**), mp 91° (86-89°); 6aβ,12aβ-rotenolone (**IIA**), mp 80-81° (80°); 6aα,12aα-rotenolone (**IIB**), mp 87-89° (88°); 6aα,12aβ-rotenolone (**IIC**), mp 247° (245°); 6aβ, 12aα-rotenolone (**IID**), mp 244-246° (245°); 6aβ, 12aβ-6',7'-dihydro-rotenone (**IA[H]**), mp 165-166° (164°).

Acknowledgement.

The authors thank Steve Erickson for technical assistance.

REFERENCES AND NOTES

[1] Author to whom correspondence should be directed.

[2] S. L. Abidi, paper presented at the International Symposium on Liquid Chromatography, June 1982, Philadelphia, Pennsylvania.

[3] T. J. Haley, *J. Environ. Pathol. Toxicol.*, **1**, 315 (1978) and references therein.

[4] T. Unai, *J. Pesticide Sci.*, **5**, 453 (1980).

[5] L. F. Johnson and W. C. Jankowski, "Carbon-13 NMR Spectra", Wiley-Interscience, New York, NY, 1972, pp 205-427.

[6] F. W. Wehrli and T. Wirthlin, "Interpretation of Carbon-13 NMR Spectra", Heydon, New York, NY, 1976, p 251.

[7] L. Crombie and P. J. Godin, *J. Chem. Soc.*, 2861 (1961).

[8] S. L. Abidi, *Anal. Chem.*, **54**, 510 (1982).

[9] R. L. Vold, J. S. Waugh, M. P. Klein and D. E. Phelps, *J. Chem. Phys.*, **48**, 3831 (1968).